

Transient storage processes in a steep headwater stream

Elisa B. Scordo¹ and R. Dan Moore^{2*}

¹ BGC Engineering Incorporated, Vancouver, Canada

² Department of Geography and Department of Forest Resources Management, University of British Columbia, Vancouver, Canada

Abstract:

This study examined hyporheic exchange flow and transient storage processes within a steep headwater stream, using both hydrometric and tracer approaches. Vertical hydraulic gradients varied systematically with location within step-pool units, with upwelling located in a relatively narrow zone immediately below the step. Downward hydraulic gradients were greatest immediately above channel steps, and in that zone, gradients were also correlated with step height. Hydraulic conductivity tended to be lower in downwelling zones than in upwelling and neutral locations. Transient storage areas determined from reach-scale tracer tests tended to increase with discharge, whereas transient exchange coefficients were not correlated with discharge. Transient storage exchange fluxes estimated from the reach-scale tracer tests were an order of magnitude greater than hyporheic exchange fluxes estimated by scaling up local estimates based on Darcy's Law and piezometer measurements. This difference could be explained by the presence of lateral hyporheic flow paths and/or the influences of transient storage in pools. Tracer injections into infiltrometers using Rhodamine WT and sodium chloride allowed visual determination of hyporheic discharge zones and calculation of residence times for hyporheic flow through the step (pool inflow) and transport through the downstream pool (pool outflow). These tests indicated that residence time in pools can be comparable to hyporheic residence times, although the lack of replication in time and space limits the drawing of strong inferences. Copyright © 2009 John Wiley & Sons, Ltd.

KEY WORDS hyporheic exchange flow; headwater stream; transient storage; OTIS-P; streambed infiltration; tracer

Received 18 July 2008; Accepted 25 March 2009

INTRODUCTION

Solutes in streams are subject to downstream transport by advection and dispersion, and can also be retained within a reach by transient storage processes, including hyporheic exchange and retention in pools and dead zones. In steep streams, hyporheic exchange flow is driven by variations in hydraulic head gradients resulting from in-stream structural complexity created from large woody debris (e.g. log jams) and geomorphic features such as step-pool sequences or breaks in topography (Harvey and Bencala, 1993). Variations in longitudinal gradient in step-pool and riffle-pool sequences drive small-scale exchange flow both vertically and laterally into the riparian zone (e.g. Harvey and Bencala, 1993; Vervier *et al.*, 1993; Morrice *et al.*, 1997; Hill *et al.*, 1998; Storey *et al.*, 2003; Anderson *et al.*, 2005; Gooseff *et al.*, 2006). Channel-unit features, such as side channels, meander bends, gravel bars and boulder or log-steps also drive exchange (Wondzell and Swanson, 1996).

Field-based and modelling studies of step-pool and riffle-pool channels have demonstrated that channel-unit spacing, size and sequence are important controls on exchange flow patterns (Anderson *et al.*, 2005; Gooseff *et al.*, 2006), suggesting that a scaling relation to identify zones of hyporheic discharge (i.e. upwelling or

outwelling) and recharge (i.e. downwelling) based on channel-unit geometry would be a useful tool for characterising and predicting exchange flow, as called for by Bencala (2000). However, upwelling of hyporheic water below steps in the Lookout Creek basin (Oregon, USA) has not been observed despite predictions from groundwater flow models that upwelling should occur (Anderson *et al.*, 2005; Gooseff *et al.*, 2006; Wondzell, 2006). These results suggest that hyporheic discharge may occur by different mechanisms, including lateral inflow across the banks or outwelling from the step wall.

Transient storage processes are typically studied at the reach scale using a transient storage model (TSM) consisting of a one-dimensional advection–dispersion equation with an additional term for transient storage, such as One-Dimensional Transport with Inflow and Storage (OTIS)) and OTIS-P (Bencala and Walters, 1983; Runkel, 1998). The TSM provides reach-scale estimates of the solute transport processes of advection, dispersion, transient storage and lateral inflow, by simulating the breakthrough curves (BTCs) generated from stream tracer injections (e.g. D'Angelo *et al.*, 1993; Harvey and Bencala, 1993; Morrice *et al.*, 1997; Mulholland *et al.*, 1997; Gooseff *et al.*, 2003). Solute transport processes inferred from TSM studies vary with discharge at the reach scale (e.g. Legrand-Marcq and Laudelout, 1985; D'Angelo *et al.*, 1993; Harvey *et al.*, 1996; Morrice *et al.*, 1997; Hart *et al.*, 1999; Patschke, 1999; Zarnetske *et al.*, 2007); however, conflicting responses have been reported. For example, studies have observed a decrease in transient

*Correspondence to: R. Dan Moore, Department of Geography and Department of Forest Resources Management, the University of British Columbia, 1984 West Mall, Vancouver, BC V6T 1Z2, Canada.
E-mail: rdmoore@geog.ubc.ca

storage area (A_S) and an increase in the transient storage exchange coefficient (α) with increasing discharge (D'Angelo *et al.*, 1993; Harvey *et al.*, 1996). Contrary to these findings, Hart *et al.* (1999) and Legrand-Marcq and Laudelout (1985) reported that transient storage area remained constant with discharge. Wondzell (2006) cautioned that these apparent changes in hydraulic parameters with discharge may be an artifact of the experimental method.

These conflicting results highlight the uncertainty surrounding the response of transient storage parameters to discharge in headwater streams. Part of this uncertainty has been attributed to the TSM approach, which is sensitive to experimental design (Wagner and Harvey, 1997) and parameter fitting routines (Runkel, 1998). As a result, Wondzell (2006) cautioned that TSM comparisons should be restricted to stream tracer experiments performed within different reaches of a single stream under comparable flow conditions. However, a fundamental problem in the interpretation of TSM studies is the separation of transient storage into hyporheic and surface-storage components. Gooseff *et al.* (2003) tried to disentangle these two processes by comparing results from two reaches, a bedrock reach with minimal hyporheic exchange and another dominated by hyporheic exchange. However, disentangling these processes within a single reach remains a significant research challenge. One potential approach is to combine reach-scale tracer tests with observations at the channel-unit scale, including both hydrometric and tracer approaches, as implemented by Stoffleth *et al.* (2008) in a sand-bed stream.

The overall objective of this study was to conduct hydrometric and tracer studies at both the channel unit and reach scales to shed light on the spatio-temporal variability and relative roles of hyporheic exchange and transient storage in pools in a steep headwater stream. Specific objectives were (1) to determine where zones of hyporheic discharge and recharge are located within the stream channel; (2) to develop empirical relations between hydraulic gradients and channel-unit geometry, specifically step spacing and downstream step height; (3) to explore the differences in hydraulic conductivity between reaches and downwelling versus upwelling zones; (4) to compare estimates of hydraulic conductivity based on piezometer slug tests to values based on direct measurement of bed infiltration; (5) to document transient storage processes in pools and compare these with reach-scale estimates; (6) to examine how solute transport processes vary with discharge; and (7) to attempt to scale up water fluxes calculated at the local scale to estimate reach-scale hyporheic exchange.

METHODS

Study site

This study was conducted within a 100 m section of East Creek, a second-order stream draining a 100 ha catchment located in the University of British Columbia

Malcolm Knapp Research Forest (MKRF) (49°16' N, 122°34' W; Figure 1). The area has a maritime climate with wet mild winters and warm dry summers. Mean annual precipitation at the University of British Columbia Research Forest headquarters (147 m elevation) is 2184 mm (Environment Canada, 1993), of which 70% falls, primarily as rain, between October and April due to Pacific frontal systems. Snowfall comprises only 5% of the total annual precipitation at the headquarters. Streamflow typically responds rapidly to rainfall. Periods of low flow dominate during the summer months (base flow <1 l/s). Runoff generation processes are dominated by subsurface flow and, to a lesser extent, saturation overland flow (Thompson and Moore, 1996; Hutchinson and Moore, 2000).

Soils within the catchment are dominantly highly permeable podzols formed from glacial till, averaging about 1 m deep and underlain by basal till over granitic bedrock (Klinka and Krajina, 1986). In some locations, the soils directly overlie bedrock.

Vegetation along East Creek is dominated by Douglas-fir (*Pseudotsuga menziesii*) and western red cedar (*Thuja plicata*), which are approximately 130 years old. Red alder (*Alnus rubra*) occurs along the stream banks in patches. Selective forest harvesting occurred adjacent to the stream in the 1970s, but instream large wood pieces were retained in the stream. Structural complexity from in-stream large wood pieces and heterogeneous substrate deposition has contributed to the formation of distinct pool-cascade sequences with both boulder and log steps.

A large sediment dam divides the reach into two sections (upper and lower reach), each about 45 m long. Stream morphology in the upper reach consists of low gradient (approximately 4%) riffle-run and pool sequences with natural log steps, and the substrate is composed of fine to coarse gravel and medium size cobbles. The lower reach has a gradient of approximately 12% and contains pool-cascade sequences with boulder and log steps. Fine-to-medium gravels in deposition areas behind steps and large anchor cobbles and boulders contribute to a spatially heterogeneous substrate. Both reaches have bankfull widths of 2.5–3.0 m. Sediment transport processes in East Creek vary seasonally with discharge. Since 2003, approximately 10–15 sediment mobilising events per year have been observed, of which 3–4 peak rainfall events during the fall and winter months of each year move the majority of sediment (J. Caulkins, pers. comm.).

Measurements from piezometers and infiltrometers

Piezometers were installed in a dense network near the centre of the stream channel at multiple depths (0–15, 15–30, 30–50 cm) both parallel and perpendicular to the main axis of the wetted stream channel (Figure 1). Two types of stream bed piezometers were used: aluminum piezometers for taking water chemistry samples and measuring hydraulic gradients ($n = 28$) and plastic piezometers to measure hydraulic gradients and hydraulic

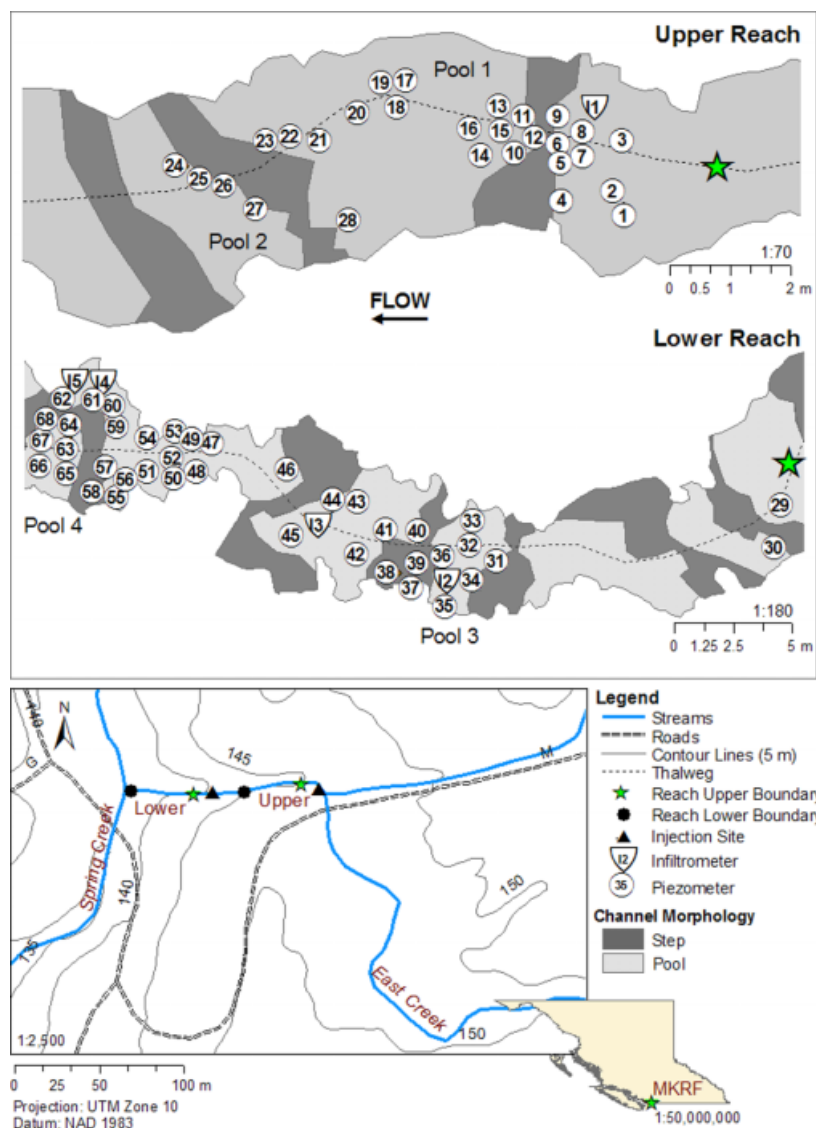


Figure 1. Study location within the East Creek catchment of the University of British Columbia Malcolm Knapp Research Forest

conductivity ($n = 41$). Plastic piezometers consisted of a 0.7 cm inside diameter (i.d.) PVC pipe, 60 cm in length, with a 5 cm slot zone screened with nylon mesh. Aluminum piezometers were constructed using a 1 cm i.d. aluminum tube, approximately 60 cm in length, with a slot zone of 5 cm. The location and elevation of all piezometers were surveyed using a Leica Geosystems total station.

Water levels in the piezometers were measured using a ‘dip stick’ with electrical contacts on the lower end, connected to a buzzer that sounded when the contacts reached a water surface. Vertical hydraulic gradients (VHG, cm cm^{-1}) in the streambed were calculated as follows:

$$\text{VHG} = \frac{\Delta h}{\Delta l}, \quad (1)$$

where Δh is the elevation of the water in the piezometer minus the elevation of the stream water surface (cm), and Δl is the distance between the surface of the stream bed and the middle of the slot zone (cm) (Baxter *et al.*, 2003). Positive VHG indicates upwelling hyporheic or

groundwater; negative VHG indicates downwelling flow. Neutral piezometers were defined as having $|\text{VHG}| < 0.05 \text{ cm cm}^{-1}$, which bounds the uncertainty of VHG measurements (Guenther, 2007).

Piezometers were also used to measure saturated hydraulic conductivity of the bed sediments using a falling head slug test (Freeze and Cherry, 1979). Hydraulic conductivity (K) was computed based on an equation derived by Hvorslev (1951) and modified by Baxter *et al.* (2003) for closed-bottom perforated piezometers.

Direct measurements of stream bed infiltration rates (IRs) were conducted using constant-head infiltrimeters constructed from ~ 20 cm long sections of 7.5 cm i.d. PVC pipe. A hole drilled into the PVC pipe at mid length was used to connect the pipe to a Mariotte cylinder using a piece of tygon tubing (Figure 2). The PVC pipe was installed into the stream bed such that the mid-length opening to the PVC pipe was level with the stream bed. The Mariotte cylinders maintained a constant head in the infiltrimeters. Infiltrimeters were installed into

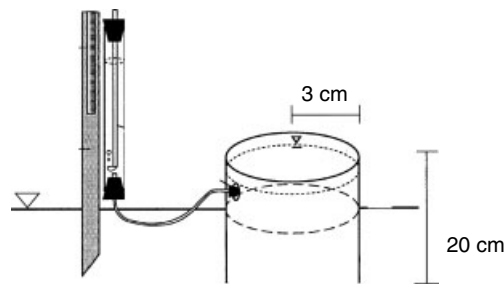


Figure 2. Streambed infiltrmeter. Adapted from Martin (1996)

the stream bed in five downwelling locations (Figure 1). Given the coarse nature of the stream bed, we were only able to install the infiltrmeters in areas where the bed was dominantly sand and fine gravel to maximise the likelihood that we could achieve a good seal while minimising disturbance to the stream bed. During operation, we maintained the water level within the infiltrmeter to be slightly lower than outside to avoid having a hydraulic gradient that could drive leakage and thus overestimate the IRs. Consequently, if there is any bias in the measurements, it would tend to be in the direction of underestimating infiltration. During all infiltrmeter measurements, water velocities in the stream channel were sufficiently low that the infiltrmeter did not visibly alter flow velocity or stage.

The IR was calculated as follows:

$$\text{IR} = \frac{\Delta h \pi(r_1^2 - r_2^2)}{\Delta t \pi(r_i^2)}, \quad (2)$$

where Δh is the change in water level in the Mariotte tube (cm) during an interval; Δt (s); r_1 , r_2 and r_i are the inside radius of the Mariotte reservoir (cm), the outside radius of the bubbler tube in the Mariotte reservoir (cm) and the inside radius of the infiltrmeter tube (cm), respectively. Uncertainties in the IRs were computed by standard equations for propagation of probable errors, based on estimated probable errors in the measured quantities (h , Δt , r_1 , r_2 and r_i). A piezometer was co-located with each infiltrmeter to allow estimation of hydraulic conductivity as $K_{\text{inf}} = \text{IR} \div |\text{VHG}|$.

Modelling spatial patterns of VHG

Measured VHG was used to map zones of hyporheic discharge (upwelling) and recharge (downwelling) along the stream profile in ArcGIS version 9.1. A geometric scaling relation was developed to describe gradients as a function of location in the stream channel. The general form of the hypothesised relation is:

$$\text{VHG} = f\left(\frac{X}{L}, \text{SH}\right), \quad (3)$$

where X is the distance from the upstream end of the pool to the piezometer (m), L is the distance from the upstream end of the pool to the edge of the step downstream of the pool (m) and SH is the height of the downstream step (m), as defined by Zimmermann

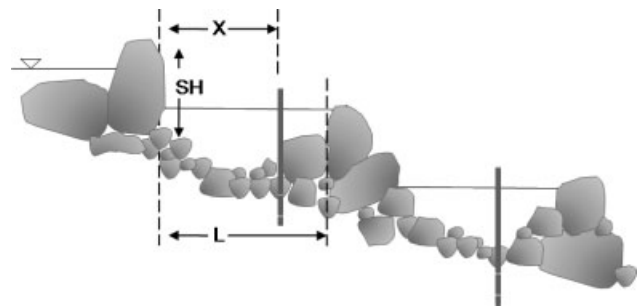


Figure 3. Geometric scaling relationship between step height (SH), the distance from the upstream end of the pool to the piezometer (X) and the distance from the upstream end of the pool to the edge of the step downstream of the pool (L)

and Church (2001) and shown in Figure 3. It was hypothesised that VHG should be negatively related to X/L , with positive gradients (upwelling flow) for values near 0 and increasingly negative gradients as X/L approaches 1. Furthermore, it was hypothesised that hydraulic gradients in the downwelling zone should be negatively associated with SH. That is, higher steps should exhibit stronger downwelling gradients. A total of seven channel units were used for the analysis.

Statistical analysis

Spearman's rank correlation coefficient (r_s) (Kutner *et al.*, 2004) was used to examine whether VHG and IR at each site varied with discharge. Spearman's correlation coefficient was also used to compare the relationship between hydraulic retention time and channel friction factor.

A linear mixed-effects model (Maindonald and Braun, 2007) was used to examine the spatial variability in hydraulic gradients and hydraulic conductivity using the 'lme4' function in R 2.7.1 for unbalanced experimental designs (R Development Core Team, 2007). A mixed-effects model was necessary to accommodate the hierarchical structure of the data; piezometers were nested within step-pool units, and thus do not represent fully independent observations due to the possibility of intra-unit correlation. In the linear models, the response variables were the mean hydraulic gradient or hydraulic conductivity for each piezometer. In the models for hydraulic gradient, predictor variables included step height, channel position and channel unit. Channel position was coded as a factor, with levels based on the following intervals for X/L : 0.0–0.2, 0.2–0.4, 0.4–0.6, 0.6–0.8 and 0.8–1.0. Channel unit was considered a random effect ($n = 7$) as we wanted to draw inferences beyond the specific units studied, whereas SH and channel position (five levels) were fixed effects.

In the model for hydraulic conductivities, predictor variables included channel unit (random) and flow direction (upwelling, neutral and downwelling; fixed). Hydraulic conductivities were log transformed before analysis. A significance level of 0.05 was used for all analyses.

Channel-unit tracer injections

Tracer injection experiments involving Rhodamine WT (RWT) were conducted at three infiltrometers to identify visually the location of hyporheic discharge within individual channel units. Injection experiments were conducted at infiltrometers I-4 and I-5 in the lower reach on six occasions (July 11, August 14, August 21, September 27/28 and October 6) as well as at infiltrometer I-1 in the upper reach on four dates (July 12, August 23, September 28 and October 6). Locations of infiltrometers are shown in Figure 1.

Sodium chloride (NaCl) was injected into infiltrometer I-5 to quantify separate residence time distributions within the hyporheic and pool storage zones on four occasions. A solution of 1 l deionised water and 20 g of salt was added directly to the infiltrometer at the rate of infiltration. Electrical conductivity (EC) was monitored around the infiltrometer to ensure that no solution was leaking through the streambed sediments. EC was continuously measured at two locations within the downstream pool using WTW conductivity probes. One probe was installed 2.5 m downstream from the injection site at the start of the pool (or pool inflow) along with a second probe installed a further 2.2 m downstream at the end of the pool (or pool outflow). Both probes were installed at the water–streambed interface adjacent to piezometers 68 and 66, respectively. Because EC increases linearly with salt concentration, it is an economical alternative to direct measurements of chloride (Gooseff and McGlynn, 2005; Wondzell, 2006). The DIN 19266 non-linear calibration built into the WTW meter was used to correct the EC values to a standard temperature of 25 °C. Injections were performed on four dates.

The mean residence time (MRT) for hyporheic flow through the step was estimated by finding the location of the centre of mass of the BTC at the start of the pool, assuming that the tracer input could be treated as being instantaneous. To estimate MRT within the pool, a simple approach based on linear reservoir theory was applied, which assumes that the pool behaves as a continuously stirred tank reactor (CSTR) (Chapra, 1997). Complete mixing of the solute and steady-state water flow for the duration of the tracer injection experiment were assumed. A mass balance for the pool can be expressed as follows:

$$\frac{dM(t)}{dt} = q_{in}(t) - q_{out}(t), \quad (4)$$

where $M(t)$ is the mass of tracer in pool (kg), $q_{in}(t)$ is the input of tracer (kg/s) and $q_{out}(t)$ is the output (kg/s). Mass can be related to tracer concentration using the equations:

$$M(t) = V \times c(t), \quad (5)$$

$$q_{out}(t) = Q \times c_{out}(t), \quad (6)$$

where V is the volume of water in pool (m^3), $c(t)$ is the concentration of tracer in the pool at time t (kg/m^3), Q is the water discharge at the outlet of the pool (m^3/s)

and $c_{out}(t)$ is the tracer concentration at the outlet. Using CSTR theory, the MRT of solutes within the system can be expressed as:

$$MRT = \frac{V}{Q} = \frac{1}{k}, \quad (7)$$

where k is a first-order exchange coefficient (s^{-1}). Towards the end of the experiment, tracer discharge to the pool will become small, and the relationship between concentration and time can be modelled as a first-order reaction:

$$\frac{dc(t)}{dt} = -k \times c(t). \quad (8)$$

Integrating Equation (8), subject to the initial condition $c(t_0) = c_0$, yields:

$$c(t) = c_0 e^{-k(t-t_0)}, \quad (9)$$

where c_0 is the concentration at time $= t_0$, which is an arbitrarily selected time. Equation (9) can be transformed by taking logarithms of both sides to yield:

$$\ln[c(t)] = \ln[c_0] - k(t - t_0). \quad (10)$$

If a plot of the logarithm of concentration against time yields a straight line, Equation (10) holds true, and k can be calculated as the slope of a straight line fitted to the linear portion of the log-transformed BTC.

Stream tracer injections

Stream tracer experiments were conducted to compare solute transport processes within the morphologically distinct upper and lower reaches. BTCs were sampled at upper and lower reach boundaries. Solute injections occurred far enough upstream of the upper sampling location to ensure full mixing (Figure 1). Sample locations were the same for all flow conditions. However, during higher flow conditions ($Q > 10$ l/s), the upper reach injection point was used to generate BTCs for both study reaches; at lower flows, separate injections were performed for the two reaches. A concentrated solution of NaCl was added at a constant rate using a Mariotte bottle consisting of a 30 l carboy (Moore, 2004a). During low flow conditions (Aug 11 to Oct 23), a battery-operated Solinst Model 410 peristaltic pump was used to conduct longer duration injections.

Streamwater EC was measured as a surrogate for tracer concentration during stream tracer tests using WTW conductivity meters (models 340, 340i and 350i). The LF340 and 340i WTW conductivity meters were attached to a Campbell Scientific CR510 data logger to record measurements. EC values measured using the WTW 350i meter were recorded to the meter's internal memory. All instruments logged EC every 30 s.

Tracer was injected until a steady-state plateau was reached (Stream Solute Workshop, 1990). Once steady-state was achieved, as determined as a constant conductivity reading for more than 10 min at the farthest downstream location, the injection was stopped and conductivity recordings continued until the stream water returned to background.

Conductivity meters were also placed at the inflow and outflow location of three pool sub-units during two reach-scale tracer injections (September 29, 30). BTCs from two pools located in the upper reach (Pool 1, 2) and one pool (Pool 3) located in the lower reach were used to quantify pool storage and residence time (Figure 1). Each pool was simulated as a distinct 'reach' using OTIS-P (Runkel, 1998).

Streamflow and lateral inflows

Streamflow was calculated at the reach boundaries using the plateau EC reading following the approach used in constant-rate salt injection (Moore, 2004b). Lateral inflow rates were estimated as the difference in discharge measured at the upstream and downstream sampling locations (Figure 1):

$$Q_L = \frac{Q_{ds} - Q_{us}}{L_r}, \quad (11)$$

where Q_L is the net lateral inflow rate ($l\ s^{-1}\ m^{-1}$), Q_{ds} and Q_{us} are streamflow (l/s) measured at the downstream and upstream locations within the reach, respectively and L_r is the reach length (m).

Transient storage modelling

BTCs generated from stream tracer experiments conducted at the reach scale and the scale of individual pools were analysed using OTIS-P. The model uses a non-linear least squares method to determine optimal parameter values for main channel cross-sectional area (A , m^2), transient storage zone cross-sectional area (A_s , m^2), longitudinal dispersion coefficient (D , $m^2\ s^{-1}$) and the transient storage zone exchange coefficient (α , s^{-1}).

Model parameters estimated using OTIS-P were used to derive the following quantities to allow comparison between the reaches: (1) hydraulic uptake length (Mulholland *et al.*, 1997), (2) hydraulic residence time (or contact time) in the storage zone and stream (Thackston and Schnelle, 1970), (3) the hydraulic retention factor

(Morrice *et al.*, 1997), (4) the standardised storage zone area (Stream Solute Workshop, 1990; D'Angelo *et al.*, 1993), (5) the Darcy-Weisbach friction factor (Harvey *et al.* 2003) and (6) the fraction of median travel time due to storage ($\%F_{med}^{200}$, Runkel, 2002) using equations summarised in Table I. The standardised storage zone area (A_s/A) is the ratio of storage cross-sectional area to stream cross-sectional area and is the mathematical equivalent of the ratio of storage zone and stream residence times.

The Damkohler number (DaI) was computed to provide insight into the information content of the BTCs:

$$DaI = \frac{\alpha(1 + A/A_s)L}{u}, \quad (12)$$

where L is length of the stream reach (m). Wagner and Harvey (1997) showed that when DaI deviates from 1.0, the uncertainty in the modelled parameters increases. High values may occur because exchange with the streambed is relatively fast compared with the water velocity or the reach length may be too long. Small DaI (<0.1) could result from (1) high stream velocity, (2) long exchange time scale as indicated by a low α and A_s/A ratio and/or (3) too short a reach length.

Scaling local bed infiltration estimates to the stream reach

Vertical flux rates were calculated by multiplying the geometric mean hydraulic conductivity for each piezometer ($n = 2-6$ observations) by the hydraulic gradient for several observation dates (June 19, Sept 21, Sept 30 and Oct 20). A linear relation was fitted between the computed vertical flux and X/L for each date and stream reach. These relations were used to scale up local fluxes to the channel reach by, first, mapping contours of X/L at intervals of 0.2 and determining the areas of the stream bed between pairs of contours. For intervals of X/L where downwelling into the bed occurred ($X/L = 0.4-0.6, 0.6-0.8, 0.8-1.0$), the predicted flux rate associated with the median value of X/L for each

Table I. Derived quantities from transient storage model parameters

Parameter	Metric	Units	Citation
Storage zone residence times (T_{stor})	$\frac{A_s}{A\alpha}$	min	Thackston and Schnelle (1970)
Stream residence times (T_{str})	$\frac{1}{\alpha}$	min	Thackston and Schnelle (1970)
Uptake length (S_{hyd})	$\frac{Q}{A\alpha}$	m	Mulholland <i>et al.</i> (1997)
Retention factor (R_h)	$\frac{T_{stor}}{S_{hyd}}$	sm^{-1}	Morrice <i>et al.</i> (1997)
Standardised storage zone area	$\frac{A_s}{A}$	—	Stream Solute Workshop (1990) and D'Angelo <i>et al.</i> (1993)
Storage exchange flux (q_s)	αA	m^2/s	Harvey <i>et al.</i> (1996) and Harvey and Wagner (2000)
Darcy-Weisbach friction factor (f)	$\frac{8gds}{u^2}$		Harvey <i>et al.</i> (2003)
Fraction of median travel time down a 200 m reach due to transient storage ($\%F_{med}^{200}$)	$\frac{t_{med} - t_{med, main}}{t_{med}}$	%	Runkel (2002) and Lautz and Siegel (2007)

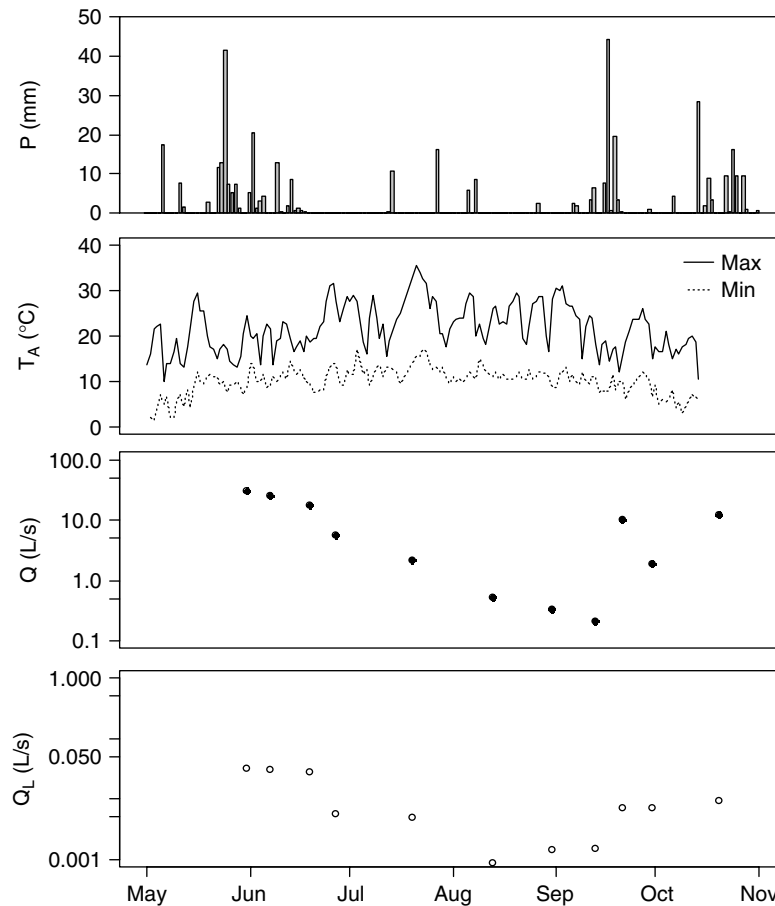


Figure 4. Daily precipitation, maximum and minimum daily temperatures, measured discharge and net lateral inflow from tracer injections conducted during the study period of May to October 2006. Discharge values represent streamflow measured at the lower reach boundary. Note log scale for Q and Q_L . Climate data recorded at the Haney-University of British Columbia Research Forest Admin climate station (Environment Canada)

category (i.e. 0.5, 0.7 and 0.9) was multiplied by the contributing area (m^2) for the category; these fluxes were then summed to yield a channel-unit flux rate (m^3/s). Three channel units per reach were analysed. The total water flux (m^2/s) into the streambed at the local scale was calculated as the sum of all channel-unit water fluxes ($n = 3$) divided by the reach length (50 m). The total scaled flux was compared with reach-scale estimates of transient storage exchange derived from OTIS-P (m^2/s).

RESULTS

Study period overview

The study period was warmer and drier than the 30 year norm. Stream tracer experiments were conducted from May 31 to October 20, 2006. Measured streamflow ranged from 0.21 l/s on September 13 to 30.6 l/s on May 31 (Figure 4). Discharges were too high by early November (>200 l/s) to continue the study. Uncertainties in measured discharge varied between 3 and 7% for all flow conditions. BTCs were modelled using OTIS-P only for tracer injections where both the upper and lower reach boundary concentrations reached plateau ($n = 10$).

Hydraulic gradients, hydraulic conductivity and bed infiltration

Strong negative hydraulic gradients typically occurred immediately upstream of a step or riffle indicating infiltration into the stream bed. Zones of hyporheic discharge, or upwelling (as indicated by a positive VHG), were confined to the upper portion of the step-pool units ($X/L = 0.0$ to 0.4). For $X/L > 0.2$, there was a trend to increasingly negative hydraulic gradients with increasing distance from the head of the channel unit (Figure 5).

A sequential analysis of variance using three linear mixed-effects models confirmed that position within the stream channel (as defined by the category of X/L) explained a significant fraction of the observed variability in hydraulic gradients (Table II). The addition of downstream step-height to the base model, which included channel unit as a random effect, did not significantly improve the model (Table II). Examination of Figure 5 suggests that VHG is negatively correlated with SH only for X/L between 0.8 and 1.0, i.e. immediately upstream of the step. A mixed-model analysis including data only for that category of X/L confirmed the significance of the negative relation, which had a slope of -0.74 m^{-1} ($p = 3 \times 10^{-6}$); that is, the hydraulic gradient would change by -0.074 m/m for each 10 cm increase in height.

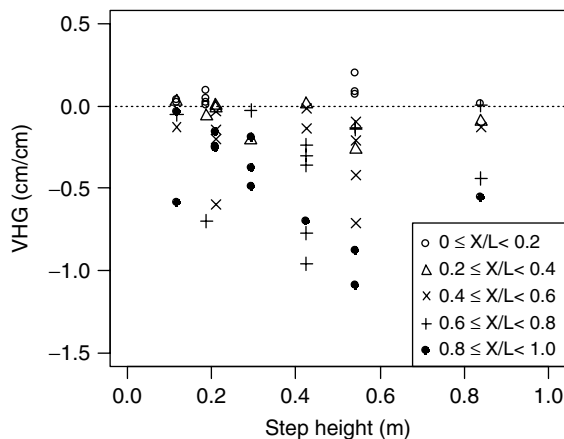


Figure 5. Vertical hydraulic gradients versus step height (m) as a function of scaled location within the channel unit (X/L)

Table II. Analysis of variance table comparing three linear mixed-effects models for vertical hydraulic gradients

Model	DF	χ^2	DF χ^2	p Value
Unit	3			
Unit + X/L	7	26.9	4	2×10^{-5}
Unit + X/L + SH	13	0.9	6	1

Note: The three models are a base model with only channel unit, a second model with channel-unit and step height (SH) and a third model with channel unit, step-height and channel position (X/L). A chi-square (χ^2) statistic was used to test for significance

The geometric means of conductivities for the lower and upper reaches were 2.54×10^{-4} ($n = 24$) and 2.37×10^{-4} m/s ($n = 17$), respectively. Conductivities appeared to be higher at neutral and upwelling sites than at downwelling sites in the lower reach (Figure 6); however, only three sites in the analysis were considered upwelling sites, compared with downwelling ($n = 21$) and neutral sites ($n = 17$). A sequential analysis of variance using two linear mixed-effects models confirmed that flow direction significantly contributed to the observed variability in hydraulic conductivity ($\chi^2 = 6.7$, $p = 0.01$, Table III).

IRs and VHGs varied considerably through time (Figure 7). As expected from Darcy's law, IRs were positively correlated with |VHG|, although with substantial scatter due, in part, to measurement uncertainty (Figure 7). The probable errors for infiltration measurements ranged up to $\pm 60\%$ of the measured value. During the lowest flow conditions, the stream water level

Table III. Analysis of variance table comparing two linear mixed-effects models for hydraulic conductivity (log transformed)

Model	DF	χ^2	DF χ^2	p Value
Reach	2			
Reach + Flow direction	3	6.7	1	0.01

Note: The models compared are a base model with only reach as a factor and a second model with reach and flow direction (upwelling, neutral and downwelling). Reach ($n = 2$) was considered a random effect, whereas flow direction was a fixed effect

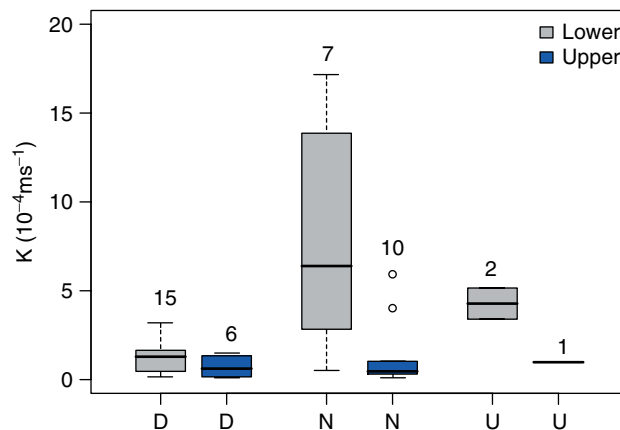


Figure 6. Hydraulic conductivity (K) for downwelling (D), neutral (N) and upwelling (U) sites located in the lower ($n = 24$) and upper reach ($n = 17$). Numbers above each box represent the sample size. Boxes represent the lower quartile, median and upper quartile. Whiskers represent the largest and smallest non-outlier observations. Data points above or below whiskers represent outliers

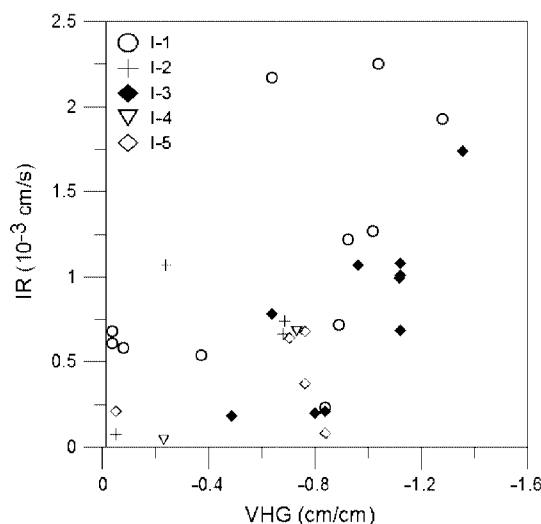


Figure 7. Infiltration rates versus vertical hydraulic gradient

dropped below the minimum level of the bubbler tube in the Mariotte reservoir, so that we could not maintain the water level within the infiltrometer at the same level as in the stream. These conditions resulted in a lack of observations during mid-to-late August. In two locations, IRs were significantly correlated with discharge (Table IV), including the sediment step (I-3) and boulder step (I-5). The boulder step (I-5) location also had the strongest mean VHG (-1.1 cm cm $^{-1}$). Hydraulic conductivities computed from IRs were similar to or up to an order of magnitude lower than those computed from co-located piezometers (Figure 8).

Tracer injections into infiltrometers

Two different flow pathways were observed within one channel unit in the lower reach using RWT as a visual tracer. During two trials (July 11 and Aug 14) at infiltrometer I-5, RWT infiltrated the bed at the top of the step, travelled laterally around a large anchor boulder in the riparian zone and returned to the stream at the base

of the step within 5–10 min post-injection. During an injection trial on Sept 27, RWT infiltrated the streambed, travelled vertically through the step and returned to the stream at the start of the pool. RWT was visible in the pool within 9 min, and was still slightly visible within the pool after 1 h. Vertical hyporheic flow pathways were also observed at another boulder step channel-unit in the lower reach (I-4). Hyporheic discharge was not observed during trials at a log-step channel unit in the upper reach (I-1), suggesting the presence of much slower flow or much longer subsurface flow paths.

Only two of the four salt injections into infiltrometer I-5 yielded ‘clean’ BTCs, with similar areas under the curves for both the pool inflow and pool outflow. The other two yielded BTCs with differing areas. We assumed that during those trials, the EC probe was not properly positioned to record the BTC at the upstream end of the pool, and the curves were not analysed further. Following injection, the EC increased rapidly to a peak concentration at the pool inflow and pool outflow. Additional minor peaks in EC are visible on the rising and recession limbs of the BTCs for each experiment (Figure 9). These peaks could indicate separate flow pathways with different residence times within the channel unit. The pool behaved like a CSTR during the later recession portion of the BTC, as indicated by a straightening of the BTC when EC as measured during tracer injections (EC_t) and corrected for background conductivity (EC_{bg}) was plotted on a logarithmic scale (Figure 9).

Table IV. Spearman correlation coefficient (r_s), associated p values and number of observations (n) for infiltration rates versus discharge at each infiltrometer location

Location	r_s	p Value	n
Log step (I-1)	0.37	0.21	13
Sediment step (I-3)	0.92	0.01	5
Boulder step (I-4)	0.51	0.25	6
Boulder step (I-5)	0.83	0.01	7

Note: Analysis not conducted for I-2 due to insufficient observations.

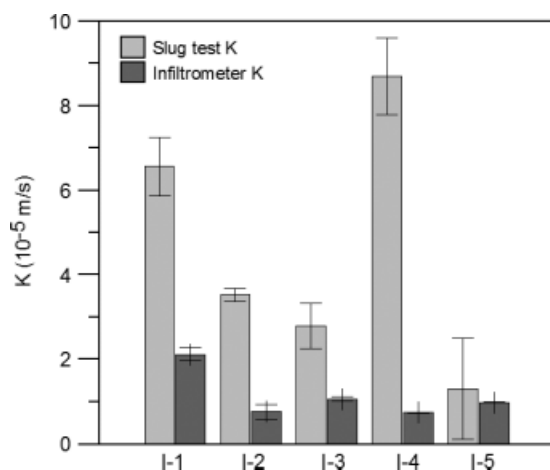


Figure 8. Hydraulic conductivity calculated using infiltration rates and slug-tests for five locations. Values represent the geometric mean \pm standard error

Table V. Mean residence times for the pool inflow (hyporheic zone) and pool storage zones in Pool 4. Vertical hydraulic gradients (VHG) measured using piezometer 61

Date	Q ($l\ s^{-1}$)	VHG (cm/cm)	Mean residence time (min)	
			Pool inflow	Pool outflow
September 25	2.4	-0.96	23.8	26.4
October 5	1.4	-0.89	68.8	71.2

MRTs varied among the experiments (Table V). For each trial, MRT was similar for the pool inflow (hyporheic zone) and pool outflow (surface storage). For both the pool inflow and pool outflow, MRT appears to vary inversely with discharge.

Reach-scale tracer injections

With the exception of the May 31 trial, which had the highest discharge at 30.6 l/s, DaI ranged from about 0.1 to 0.5 and generally decreased with discharge (Table VI), suggesting that the reach length is reasonable. Lateral inflow rates increased with discharge (Table VI), but represented less than a 10% gain of streamflow except when streamflow was less than 5 l/s. The dispersion coefficient, transient storage area and stream cross-sectional area generally increased with discharge (Figure 10) for both reaches. The transient exchange coefficient (α) did not vary systematically with discharge or between reaches (Figure 10). Stream velocity increased with discharge (Figure 11a) and tended to be higher in the upper reach. The standardised storage zone area also did not show a clear trend with discharge (Figure 11d). A majority of the values ranged from approximately 0.10 to 0.30, with the exception of the May 31 injection with a value of 0.62.

Hydraulic residence time in the stream was higher than in the storage zone for all tracer injections and did not appear to vary with discharge for either reach (Table VI). The average stream residence time was higher in the lower reach (109 min) compared with the upper reach (49.8 min). Storage zone residence time was also higher in the lower reach (31 min) compared with the upper reach (10.2 min). The hydraulic uptake length increased as discharge increased for both the upper and lower reach (Figure 11b). On average, the uptake length was higher in the upper reach (318 m) than the lower reach (305 m). The hydraulic retention factor showed no clear trend with discharge (Figure 11c). Channel friction factor had a positive but not statistically significant correlation with retention time ($r_s = 0.47$, $n = 10$, p value = 0.17). Transient storage accounted for 3 to 17% of the total reach travel time based on the metric $\% F_{med}^{200}$ and did not vary substantially between reaches.

For the three individual pools simulated using OTIS-P, the ratio A_S/A was greater for the pools than the stream reaches (Table VII). Storage zone residence times varied over two orders of magnitude, with higher values in the upper reach.

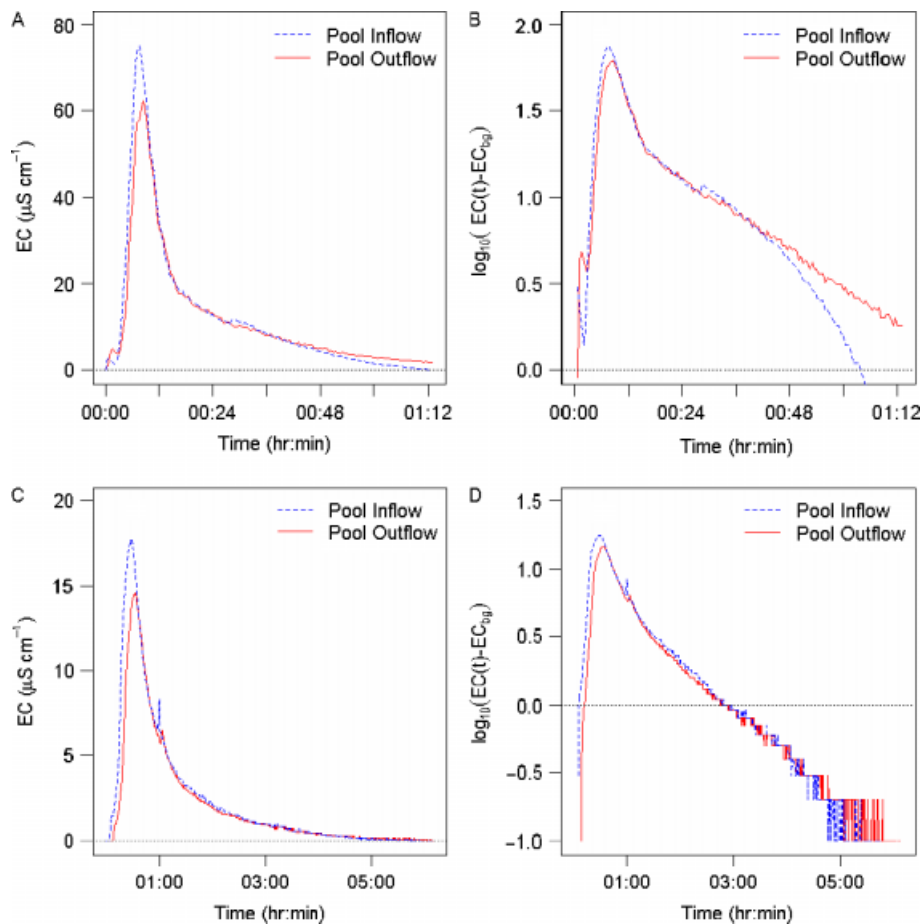


Figure 9. Step-pool breakthrough curves for tracer injections conducted in the lower reach at one location (infiltrometer I-5) on September 25 (top) and October 5 (bottom). Values plotted on a logarithmic scale represent electrical conductivity measured during tracer injections (EC_t) and corrected for background conductivity (EC_{bg})

Scaling streambed water fluxes

The relations between flux rate and X/L were not significant within the lower reach; as a result, only the upper reach was used for the analysis. Water fluxes calculated at the local scale within multiple step-pool units in the upper reach varied with flow conditions. The total computed flux into the bed was greatest during high-flow conditions on June 19 ($Q = 15.4$ l/s) compared with low-flow conditions. The reach scale estimate of transient storage exchange (q_s) was an order of magnitude greater than the scaled-up estimate of exchange fluxes for all flow conditions in the upper reach (Table VIII).

DISCUSSION

Patterns of VHGs

VHGs varied in both space and time. Consistent with previous studies, negative VHG (downwelling) was observed upstream of obstructions in the channel (i.e. steps and logs). However, unlike previous studies in Oregon (Anderson *et al.*, 2005; Gooseff *et al.*, 2006; Wondzell, 2006), positive VHG (upwelling) was clearly observed at the upstream end of pools below steps in 3 of the 41 piezometers. Other studies within the Malcolm Knapp Research Forest have made similar observations of upwelling (Patschke, 1999; Guenther, 2007).

Although upwelling was observed in locations where it was expected in East Creek, the hydraulic gradients were substantially weaker than in the downstream sections of the step-pool units (i.e. $X/L > 0.6$). Given that hyporheic exchange should be approximately at a steady state during extended periods of baseflow, upwelling and downwelling fluxes should balance. The fact that downwelling gradients were generally stronger and more spatially widespread than upwelling gradients could be explained by one or more of the following: (1) lower hydraulic conductivities in downwelling zones, (2) discharge being concentrated along preferred pathways, (3) the presence of lateral flow paths and (4) substantial discharge through the step wall. All four are possibilities at East Creek. The presence of lower conductivities in downwelling zones is consistent with observations that penetration of fine sediments into the bed (resulting in clogging of larger pore spaces) is greater in downwelling areas (Schalchli, 1992; Packman and MacKay, 2003) and is supported by the results in Figure 6. There is also some support for the presence of preferred pathways from the unit-scale tracer experiments, although it is difficult to quantify how much discharge occurred via these preferred pathways. The presence of a lateral component to hyporheic exchange is possible, particularly at some areas along the reach, but the study design did not allow the assessment

Table VI. Summary of best fit model parameters for solute releases

Reach	Q ($10^{-3} \text{ m}^3 \text{ s}^{-1}$)	Q_L ($10^{-6} \text{ m}^3 \text{ s}^{-1} \text{ m}^{-1}$)	D ($10^{-2} \text{ m}^2 \text{ s}^{-1}$)	A (10^{-2} m^2)	A_S (10^{-2} m^2)	α (10^{-4} s^{-1})	u (m s^{-1})	T_{sr} (min)	T_{stor} (min)	S_{hyd} (m)	R_h (s m^{-1})	A_S/A	RMSE (10^{-5})	DaI
Upper														
June 19	15.9	26.8	31.6	11.6	5.83	2.1	0.13	80.7	40.4	648	3.7	0.50	1.8	0.12
September 21	9.8	8.5	18.3	6.73	1.45	2.7	0.15	61.8	13.3	542	1.5	0.22	14.1	0.22
September 29	1.0	3.3	2.9	2.82	0.6	3.0	0.04	55.2	11.6	122	5.7	0.21	1.8	0.50
October 20	9.7	10.5	4.0	9.28	1.46	3.5	0.10	48.3	7.6	302	1.5	0.16	8.5	0.38
Lower														
May 31	30.6	31.8	48.6	21.7	13.5	1.4	0.14	121.5	75.7	1029	4.4	0.62	0.3	0.08
June 19	17.2	20.4	29.5	19.2	5.9	1.9	0.09	86.2	26.7	465	3.4	0.31	0.2	0.14
June 27	5.5	5.6	1.9	13.7	4.1	2.7	0.04	61.0	18.1	146	7.4	0.30	0.2	0.44
September 21	9.9	6.9	8.4	14.3	2.8	2.1	0.07	80.2	16.0	334	2.9	0.20	10.2	0.36
September 30	1.9	6.9	4.6	6.5	1.3	0.8	0.03	196.5	38.9	343	6.8	0.20	1.9	0.17
October 20	11.9	9.4	5.0	19.2	2.0	1.6	0.06	106.3	11.0	397	1.7	0.10	8.5	0.28

Note: Solute releases: Q = stream discharge; Q_L = net lateral inflow; D = dispersion coefficient; A = stream cross-sectional area; A_S = cross-sectional area of storage zone; α = storage zone exchange coefficient. RMSE = residual mean square error. Derived quantities: u = stream velocity; T_{sr} = hydraulic residence time for the stream; T_{stor} = storage zone; S_{hyd} = hydraulic uptake length; R_h = hydraulic retention factor; A_S/A = the standardized storage zone coefficient; DaI = Damkohler number

of lateral hyporheic exchange because horizontal gradients were not measured. Outwelling through the step wall was not observed during RWT injections into the steps, but cannot be ruled out as tracer tests were not conducted at all steps in the study reach.

Zones of hyporheic discharge and recharge varied systematically with position in the stream channel (as defined by X/L , Figure 5). Generally, for $X/L > 0.2$, negative hydraulic gradients increased with distance to the step. However, step height did not appear to control VGH except for piezometers immediately upstream of the step (where $X/L > 0.8$) (Figure 5). These results suggest that the relation between VGH and X/L could be a useful tool for characterising and predicting hydraulic gradients in step-pool streams, a need expressed by Bencala (2000). While channel-unit spacing, size and sequence have been identified as significant controls on exchange flow in previous studies (Anderson *et al.*, 2005; Gooseff *et al.*, 2006), the effect of step height does not appear to have previously been assessed.

The temporal variability in VGH observed at East Creek is not uncommon (Thibodeaux and Boyle, 1987; Baxter and Hauer, 2000), and could reflect discharge-controlled interactions between flow hydraulics and channel features as well as changes in hydraulic head patterns in the riparian zone. However, VGH was not correlated in a simple way with discharge at East Creek. Other processes that could influence VGH in the stream bed are changes in the wetted area and the effects of precipitation onto and evaporation from dry areas of the bed.

Solute transport parameters and discharge

In East Creek, DaI values ranged from 0.1 to 0.5 for all experiments except that with the highest streamflow as well as the results for Pool 3. Therefore, most trials were associated with DaI values in the range in which ‘well-estimated’ parameters are most likely to be obtained (Wagner and Harvey, 1997). The results of the OTIS-P simulations were in agreement with the majority of previous studies, which reported an increase in dispersion (D) and the channel cross-sectional area (A) with discharge (Legrand-Marcq and Laudelout, 1985; D’Angelo *et al.*, 1993; Harvey *et al.*, 1996; Morrice *et al.*, 1997; Hart *et al.*, 1999; Wondzell, 2006).

The transient storage area determined from the tracer tests increased with discharge. This increase is consistent with the observed increase in pool area and thus surface storage zones with discharge. In addition, increased discharge was associated with an increase in the wetted area of the channel and thus a greater area over which hyporheic recharge could occur.

The transient exchange coefficient remained fairly constant with discharge. There was some evidence of a threshold response in the lower reach, as the transient exchange coefficient increased to a plateau of $2.7 \times 10^{-4} \text{ s}^{-1}$ at 5.5 l/s and then declined with discharge. Morrice *et al.* (1997) also reported a threshold response in which α increased then decreased with discharge in

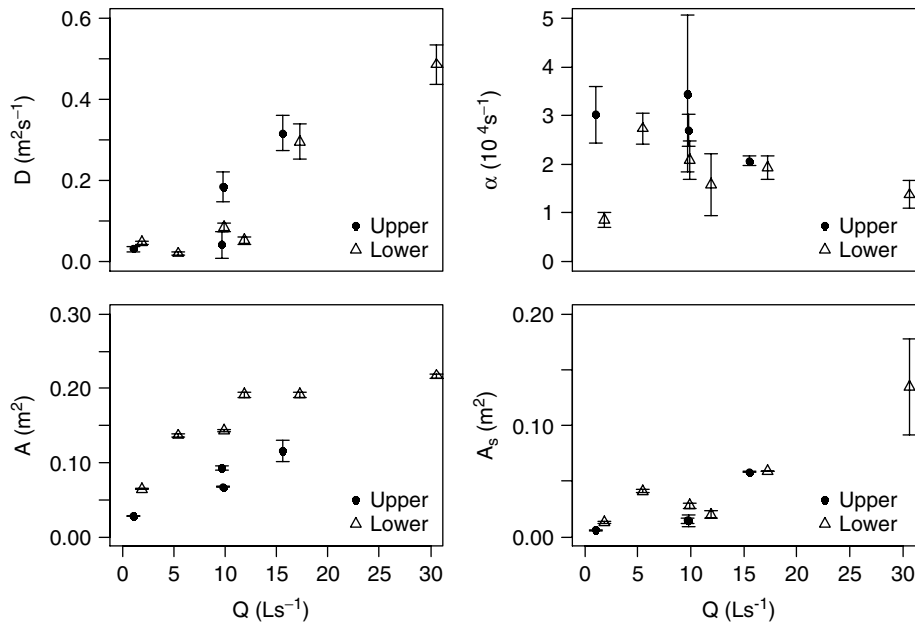


Figure 10. Simulated model parameters for solute releases in the upper and lower stream reach. Dispersion coefficient (D), stream cross-sectional area (A), cross-sectional area of storage zone (A_s), storage zone exchange coefficient (α) versus stream discharge (Q). Error bars represent ± 1 standard deviation

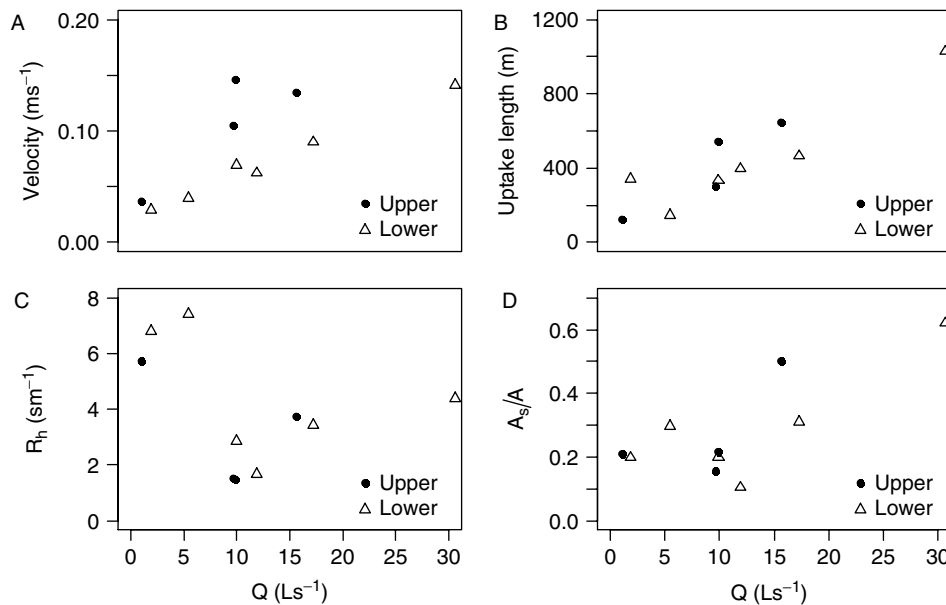


Figure 11. Stream velocity (a), hydraulic uptake length (b), hydraulic retention factor (c) and the standardised storage zone coefficient versus stream discharge (d) for the upper and lower reaches

a first-order stream. Other studies have reported either a steady increase (D'Angelo *et al.*, 1993; Harvey *et al.*, 1996; Hart *et al.*, 1999; Wondzell, 2006) or a decrease in transient exchange coefficient with discharge (Legrand-Marcq and Laudelout, 1985; Hart *et al.*, 1999; Patschke, 1999). At East Creek, this complex behaviour might be related to the changes in the extent of hyporheic recharge area in relation to the hydraulic conductivity of the bed. For example, a decrease in α could be associated with an extension of the wetted channel into areas with a low-bed conductivity or lower hydraulic gradients. Variations in α could also result from changes in the configuration of pool storage zones and their interaction with the flowing portion of the stream.

Residence times and retention

Residence times were consistently higher in the lower reach, which had greater complexity. This result is consistent with observations by Wondzell (2006) that the storage zone residence times and the hydraulic retention factor (R_h) were greater in reaches with a few large steps associated with log jams than in reaches with more frequent but smaller steps. Retention factors were comparable between the two reaches in East Creek, despite the upper reach having a greater number of log steps and a higher degree of incision. The lower reach was generally less confined than the upper reach, which may explain the longer residence times observed for transient storage.

Table VII. Summary of One-Dimensional Transport with Inflow and Storage with Parameter optimization (OTIS-P) parameter estimates of dispersion coefficient (D), stream cross-sectional area (A), cross-sectional area of storage zone (A_S) and the storage zone exchange coefficient (α) in three pools modelled as individual reaches during reach-scale tracer injections

Reach	D (10^{-2} m ² s ⁻¹)	A (10^{-2} m ²)	A_S (10^{-2} m ²)	α (10^{-4} s ⁻¹)	A_S/A	T_{str} (min)	T_{stor} (min)	DaI
September 29								
Reach 1	2.9	2.8	0.6	3.0	0.21	55.2	11.6	0.50
Pool 1	2.5	6.3	60.7	3.1	9.61	53.8	516.5	0.80
Pool 2	1.8	0.8	6.1	3.4	7.40	48.5	359.1	0.09
September 30								
Reach 2	4.6	6.5	1.3	0.85	0.20	196.5	38.9	0.17
Pool 3	8.4	2.5	5.9	145	2.33	1.2	2.7	2.60

Derived quantities included residence times in the stream (T_{str}) and storage zone (T_{stor}), the standardized storage zone coefficient (A_S/A) and the Damkohler number (DaI) for the three pools simulations compared with reach scale results

Table VIII. Scaling of transient storage exchange flux estimates from the channel unit and reach scales

Date	Q (10^{-3} m ³ s ⁻¹)	b_0 (10^{-5} m s ⁻¹)	b_1 (10^{-5} m s ⁻¹)	r^2	p Value	q_s (10^{-6} m ² s ⁻¹)	
						Darcy	OTIS-P
June 19	15.9	3.07	-11.2	0.53	0.001	4.5	24.4
September 21	9.8	1.66	-5.93	0.35	0.02	1.4	18.2
September 29	1.0	1.05	-3.25	0.27	0.04	0.6	8.5
October 20	9.7	3.59	-13.0	0.51	0.002	3.9	32.5

Q = streamflow at the lower boundary of the reach; b_0 and b_1 are the intercept and slope of a relation between vertical flux and X/L for the upper reach; r^2 and p value are the coefficient of determination and significance of the regression; q_s = reach-scale transient storage exchange flux calculated using Darcy's law and one-dimensional transport with inflow and storage (OTIS-P)

Although our ability to generalise about transient storage in the pools is limited by the small amount of replication in time and space, it appears that MRTs in pools could be a significant component of the transient storage effect modelled by OTIS-P. Therefore, one cannot safely equate modelled transient storage with storage in the hyporheic zone in streams with a steep step-pool morphology.

Scaling hyporheic exchange flow from the channel unit to the stream reach

Scaled water fluxes computed from Darcy's law within multiple channel units in the upper reach varied with flow conditions (Table VIII). Previous studies have suggested that at higher discharges (accompanied by higher stages), the hydraulic potential for downwelling into the bed increases, thus increasing the potential for hyporheic exchange flow (e.g. Wondzell, 2006). Although the scaled-up water fluxes appeared to vary with discharge, hydraulic gradients and IRs measured at the point scale did not consistently vary with discharge, as discussed above.

The 'scaled-up' hyporheic exchange flux estimates based on Darcy's law were an order of magnitude lower than the reach-scale estimates of transient storage exchange from OTIS-P (Table VIII). There are two possible explanations. First, lateral fluxes or horizontal exchange flow may have contributed to a portion of the exchange flow that was not quantified at the channel-unit scale. Second, the storage exchange flux estimated

by the TSM combines the effects of hyporheic exchange and transient storage in pools. This latter possibility is supported by our unit-scale tracer experiments, which suggest that residence times in pools can be higher than in the steps. However, the unit-scale tracer experiments had limited replication in both time and space, limiting our ability to draw strong inferences from them. These results indicate that while hyporheic exchange is not the sole or even dominant transient storage process in these two step-pool channels, it appears to play a more important role than in the sand-bed streams studied by Stoffeth *et al.* (2008), who found that hyporheic exchange determined from piezometer measurements accounted for less than 1% of the total transient storage.

CONCLUSIONS

Within step-pool units, there was a systematic pattern of VHGs, with upwelling located in a relatively narrow zone immediately below the step. Downward hydraulic gradients were greatest immediately above channel steps, and gradients in that zone were also correlated with step height. Hydraulic gradients varied in time, but did not exhibit consistent relations with discharge.

Hydraulic conductivity tended to be lower in downwelling zones than in upwelling and neutral locations. Hydraulic conductivity determined from falling head tests conducted at piezometers was similar to or somewhat

larger than values calculated from infiltrometer measurements, likely reflecting the inherent uncertainty involved in field measurements of this quantity.

Transient storage areas determined from reach-scale tracer tests tended to increase with discharge, possibly associated with the increase in wetted channel width, which would increase both pool storage and the area of hyporheic recharge. Transient exchange coefficients were not correlated with discharge, possibly due to changes in pool configuration and their interactions with the flowing portion of the channel. The lack of a clear relation between α and discharge could also reflect the spatial variation of bed hydraulic conductivity and its changing influence as the wetted portion of the stream bed increased and decreased through time.

Transient storage exchange fluxes (q_s) estimated from the reach-scale tracer tests were an order of magnitude greater than values estimated by scaling up local estimates of hyporheic recharge based on Darcy's Law and piezometer measurements. This difference could be due to one or more of the following: the apparent bias associated with the hydraulic conductivities estimated from the falling head tests, the occurrence of lateral hyporheic exchange and the role of pools.

Injections of RWT into piezometers were useful for determining visually the locations of hyporheic discharge, and revealed that the pathways may vary through time. Monitoring BTCs following injection of sodium chloride into piezometers allowed residence time distributions to be estimated separately for the pool inflow (hyporheic flow) and transient storage and transport through an individual pool. In addition, monitoring BTCs at the inlets and outlets of pools during reach-scale tracer injections provided another approach to estimating hydraulic parameters for individual pools. While there appears to be substantial variability, transient storage and MRTs in pools can be of the same magnitude as for hyporheic exchange. The analysis of channel-unit-scale tracer BTCs should be applied in future studies to help generate a better understanding of the relative roles of hyporheic exchange and within-channel transient storage.

Taken together, the results of both hydrometric and tracer observations reveal that hyporheic exchange and transient storage processes exhibit substantial variability and complex patterns in time and space. Future field studies will need to sample spatially at high resolution, and also sample a broad range of hydrologic conditions in relation to stream discharge and lateral inflow, to capture this complexity and contribute to development of predictive models (e.g. to assess the effects of changes in channel morphology). In addition, it would be valuable to conduct flume experiments to assist in isolating the various factors controlling transient storage in steep streams. Flume studies have proven valuable for studying hyporheic exchange associated with bedforms typical of lower-gradient channels (e.g. Packman and MacKay, 2003). Geomorphologists have made progress in conducting experiments to study channel stability and sediment transport in step-pool units (Curran and Wilcock, 2005;

Zimmermann *et al.*, 2008), and it would be valuable to adapt these step-pool models for quantifying transient storage processes.

ACKNOWLEDGEMENTS

The study was supported by grants to R.D.M. from the Natural Sciences and Engineering Research Council of Canada (NSERC) and Forest Investment Account (FIA), and to E.S. from an NSERC postgraduate scholarship (NSERC-CGS). The project is part of a broader FIA-funded project entitled 'Ecology and management of riparian-stream ecosystems: a large scale experiment using alternative streamside management' (P.I.: John S. Richardson). The authors greatly appreciate field support provided by T. Lagemaat, E. Morgan, J. Caulkins, A. Zimmermann, J. Leach and J. Phillips, along with support from the Malcolm Knapp Research Forest staff. M. Weiler and P. Szeftel provided constructive comments on an earlier draft of the manuscript. The comments provided by Steve Wondzell and an anonymous reviewer are greatly appreciated.

REFERENCES

- Anderson JK, Wondzell SM, Gooseff MN, Haggerty R. 2005. Patterns in stream longitudinal profiles and implications for hyporheic exchange flow at the H.J. Andrews Experimental Forest, Oregon, USA. *Hydrological Processes* **19**: 2931–2949.
- Baxter C, Hauer FR, Woessner WW. 2003. Measuring groundwater and stream water exchange: New techniques for installing minipiezometers and estimating hydraulic conductivity. *Transactions of the American Fisheries Society* **132**: 493–502.
- Baxter CV, Hauer FR. 2000. Geomorphology, hyporheic exchange, and selection of spawning habitat by bull trout (*Salvelinus confluentus*). *Canadian Journal of Fisheries and Aquatic Sciences* **57**: 170–181.
- Bencala KE. 2000. Hyporheic zone hydrological processes. *Hydrological Processes* **14**: 2797–2798.
- Bencala KE, Walters RA. 1983. Simulation of solute transport in a mountain pool-and-riffle stream: A transient storage model. *Water Resources Research* **19**: 718–724.
- Chapra SC. 1997. *Surface Water Quality Modelling*. McGraw-Hill, New York, USA. 46–85.
- Curran J, Wilcock P. 2005. Characteristic dimensions of the step-pool configuration: An experimental study. *Water Resources Research* **41**: 201–215.
- D'Angelo DJ, Webster JR, Gregory SV, Meyer JL. 1993. Transient storage in Appalachian and Cascade mountain streams as related to hydraulic characteristics. *Journal of the North American Benthological Society* **12**: 223–235.
- Environment Canada. 1993. Canadian climate normals 1961–1990. In *Atmospheric Environment Service*. Ottawa, Canada.
- Freeze RA, Cherry JA. 1979. *Groundwater*. Prentice-Hall: New Jersey, USA.
- Gooseff MN, Anderson JK, Wondzell SM, LaNier J, Haggerty R. 2006. A modelling study of hyporheic exchange pattern and the sequence, size, and spacing of stream bedforms in mountain stream networks, Oregon, USA. *Hydrological Processes* **20**: 2443–2457.
- Gooseff MN, McGlynn BL. 2005. A stream tracer technique employing ionic tracers and specific conductance data applied to the Maimai catchment, New Zealand. *Hydrological Processes* **19**: 2491–2506.
- Gooseff MN, Wondzell SM, Haggerty R, Anderson J. 2003. Comparing transient storage modeling and residence time distribution (RTD) analysis in geomorphically varied reaches in the Lookout Creek basin, Oregon, USA. *Advances in Water Resources* **26**: 925–937.
- Guenther S. 2007. *Headwater stream temperature response to alternative riparian management: An experimental heat budget approach*. Master's thesis, University of British Columbia, Vancouver, BC.

- Hart BT, Maher B, Lawrence I. 1999. New generation water quality guidelines for ecosystem protection. *Freshwater Biology* **41**: 347–359.
- Harvey JW, Bencala KE. 1993. The effect of streambed topography on surface–subsurface water exchange in mountain catchments. *Water Resources Research* **29**: 89–98.
- Harvey JW, Conklin MH, Koelsch RS. 2003. Predicting changes in hydrologic retention in an evolving semi-arid alluvial stream. *Advances in Water Resources* **26**: 939–950.
- Harvey JW, Wagner BJ. 2000. Quantifying hydrological interactions between streams and their subsurface hyporheic zones. In *Streams and Ground Waters*. Jones JB, Mulholland PJ (eds). Academic Press: San Diego, CA.
- Harvey JW, Wagner BJ, Bencala KE. 1996. Evaluating the reliability of the stream tracer approach to characterize stream–subsurface water exchange. *Water Resources Research* **32**: 2441–2451.
- Hill AR, Labadia CF, Sanmugadas K. 1998. Hyporheic zone hydrology and nitrogen dynamics in relation to the streambed topography of a N-rich stream. *Biogeochemistry* **42**: 285–310.
- Hutchinson DG, Moore RD. 2000. Throughflow variability on a forested hillslope underlain by compacted glacial till. *Hydrological Processes* **14**: 1751–1766.
- Hvorslev MJ. 1951. Time lag and soil permeability in groundwater observations. *U.S. Army Corps of Engineers, Waterways Experiment Station* 50.
- Klinka K, Krajina VJ. 1986. *Ecosystems of the University of British Columbia Research Forest, Haney, B.C.* Faculty of Forestry, the University of British Columbia: Vancouver BC.
- Kutner MH, Nachtsheim CJ, Neter J, Li W. 2004. *Applied linear statistical models* (5th ed). McGraw-Hill Irwin: New York, USA.
- Lautz LK, Siegel DI. 2007. The effect of transient storage on nitrate uptake lengths in streams: An inter-site comparison. *Hydrological Processes* **21**: 3533–3548.
- Legrand-Marcq C, Laudelout H. 1985. Longitudinal dispersion in a forest stream. *Journal of Hydrology* **78**(3–4): 317–324.
- Maindonald J, Braun WJ. 2007. *Data Analysis and Graphics Using R—An Example-Based Approach*. Cambridge University Press: Cambridge UK.
- Martin JE. 1996. *Hydrology and pore-water chemistry of a tidal marsh, Fraser River estuary*. Master's thesis, Simon Fraser University, Vancouver, BC.
- Moore RD. 2004a. Construction of a Mariotte bottle for constant-rate tracer injection into small streams. *Streamline Watershed Management Bulletin* **8**: 15–16.
- Moore RD. 2004b. Introduction to salt dilution gauging for streamflow measurements: Part 1. *Streamline Watershed Management Bulletin* **7**: 20–24.
- Morrice JA, Valett HM, Dahm CN, Campana ME. 1997. Alluvial characteristics, groundwater–surface water exchange and hydrologic retention in headwater streams. *Hydrological Processes* **11**: 253–267.
- Mulholland PJ, Marzolf ER, Webster JR, Hart DR, Hendricks SP. 1997. Evidence that hyporheic zones increase heterotrophic metabolism and phosphorus uptake in forest streams. *Limnology and Oceanography* **42**: 443–451.
- Packman AI, MacKay JS. 2003. Interplay of stream–subsurface exchange, clay particle deposition, and streambed evolution. *Water Resources Research* **39**: ESG 4-1–4-9. DOI:10.1029/2002WR001432.
- Patschke SN. 1999. *Hyporheic exchange in a forested headwater stream*. Master's thesis, Simon Fraser University, Vancouver, BC.
- R Development Core Team. 2007. *R: A Language and Environment for Statistical Computing*. R Foundation for Statistical Computing: Vienna, Austria. ISBN: 3-900051-07-0; URL <http://www.R-project.org>.
- Runkel RL. 1998. *One-dimensional transport with inflow and storage (OTIS): A solute transport model for streams and rivers*. US Geological Survey Water Resources Investigation Report 98–4018. Online: <http://pubs.er.usgs.gov/usgspubs/wri/wri984018>.
- Schalchli U. 1992. The clogging of coarse gravel river beds by fine sediment. *Hydrobiologia* **235/236**: 189–197.
- Stoffeth JM, Shields FD, Fox GA. 2008. Hyporheic and total transient storage in small, sand-bed streams. *Hydrological Processes* **22**: 1885–1894.
- Storey RG, Howard KWF, Williams DD. 2003. Factors controlling riffle-scale hyporheic exchange flows and their seasonal changes in a gaining stream: A three-dimensional groundwater flow model. *Water Resources Research* **39**: 1034. DOI: 10.1029/2002WR001367.
- Stream Solute Workshop. 1990. Concepts and methods for assessing solute dynamics in stream ecosystems. *Journal of North American Benthological Society* **9**: 95–119.
- Thackston EL, Schnelle KB. 1970. Predicting effects of dead zones on stream mixing. *Journal of the Sanitary Engineering Division* **96**: 319–331.
- Thibodeaux LJ, Boyle JD. 1987. Bedform-generated convective transport in bottom sediment. *Nature* **325**: 341–343.
- Thompson JC, Moore RD. 1996. Relations between topography and water table depth in a shallow forest soil. *Hydrological Processes* **10**: 1513–1525.
- Vervier P, Gibert J, Marmonier P, Dole-Olivier MJ. 1993. A perspective on the permeability of the surface freshwater–groundwater ecotone. *Journal of the North American Benthological Society* **11**: 93–102.
- Wagner BJ, Harvey JW. 1997. Experimental design for estimating parameters of rate-limited mass transfer: Analysis of stream tracer studies. *Water Resources Research* **33**: 1731–1741.
- Wondzell SM, Swanson FJ. 1996. Seasonal and storm dynamics of the hyporheic zone of a 4th-order mountain stream I: Hydrological Processes. *Journal of the North American Benthological Society* **15**: 3–19.
- Wondzell SM. 2006. Effect of morphology and discharge on hyporheic exchange flows in two small streams in the Cascade Mountains of Oregon, USA. *Hydrological Processes* **20**: 267–287.
- Zarnetske JP, Gooseff MN, Brosten TR, Bradford JH, McNamara JP, Bowden WB. 2007. Transient storage as a function of geomorphology, discharge, and permafrost active layer conditions in Arctic tundra streams. *Water Resources Research* **43**: W07410. DOI: 10.1029/2005WR004816.
- Zimmermann A, Church M. 2001. Channel morphology, gradient profiles and bed stresses during flood in a step-pool channel. *Geomorphology* **40**: 311–327.
- Zimmermann A, Church M, Hassan MA. 2008. Identification of steps and pools from stream longitudinal profile data. *Geomorphology* **102**: 395–406.